Synthesis and Characterization of Polymer-Templated Mesoporous Silicas Containing Niobium

Izabela Nowak,[†,‡] Maria Ziolek,[‡] and Mietek Jaroniec*[,†]

Kent State University, Department of Chemistry, Kent, Ohio 44240, and A. Mickiewicz University, Faculty of Chemistry, Grunwaldzka 6, PL-60-780 Poznan, Poland

A series of niobium-containing mesoporous silicas (Nb–MS) with different pore diameters has been synthesized via an acid-mediated route by using different kinds of nonionic triblock copolymers. The effect of the chain length of poly(propylene oxide) (PO) and poly(ethylene oxide) (EO) units on the structure of Nb–MS materials has been studied. The samples were characterized by X-ray diffraction (XRD), nitrogen adsorption, transmission electron microscopy (TEM), and temperature-programmed reduction (TPR). The pore diameter of Nb–MS increased with increasing the PO chain length in triblock copolymer. The microporosity was not affected by the type of the copolymer used.

Introduction

In 1992, Mobil scientists discovered that ionic surfactants could be used as templates for the synthesis of ordered mesoporous silicas (OMSs), which they called M41S.[1] A new type of OMSs is the SBA-15 silica with a two-dimensional (2D) hexagonal arrangement of uniform mesopores, which was synthesized by using a nonionic block copolymer as the template instead of a cationic surfactant.[2] Initially, SBA-15 was considered as an extra-large-pore MCM-41 analogue with a honeycomb structure of disconnected channel-like pores.[2] Later, much evidence was provided about the presence of interconnecting disordered micropores in SBA-15.[3,4] Currently, it is commonly accepted that SBA-15 possesses a bimodal distribution of pores, i.e., hexagonally ordered mesopores as well as micropores existing in the mesopore walls, which is highly beneficial for catalysis and adsorption because complementary micropores facilitate migration of molecules between ordered mesopores. Therefore, the synthesis of SBA-15 materials has recently attracted much attention, especially those with incorporated catalytically active species.

Up to now, only titanium[5–7] and zirconium[8] were incorporated into SBA-15 by direct syntheses and iron and aluminum by two-step procedures.[9,10] It is difficult to prepare SBA-15 containing heteroatoms in the framework due to the strong acidic synthesis conditions (pH $\ll$ 1). Such conditions are unfavorable for the formation of oxo-species that may facilitate the incorporation of transition metals into the SBA-15 framework. For the first time, this work reports the niobium-containing mesoporous silicas (Nb–MS), which were synthesized by using different triblock copolymers such as L43, L64, P94, P103, P105, and P123 (Pluronics from BASF Corp.) as templates. The Nb–MS samples templated by Pluronics with higher molecular weight exhibited an ordered mesostructure of the SBA-15 type. These polymeric templates have a general formula HO(EO)$_x$-(PO)$_y$(EO)$_x$H, in which each poly(propylene oxide) (PO) block is sandwiched between two poly(ethylene oxide) (EO) blocks. The alphabetical designation of Pluronics explains the physical form of the product: "L" is used for liquids and "P" is used for

pastes. The first digit (two digits in a three-digit number) in the numerical designation, multiplied by 300, indicates the approximate molecular weight of the hydrophobe, i.e., polypropylene oxide, whereas the last digit, when multiplied by 10, indicates the approximate poly(ethylene oxide) content (percentage) in the molecule. Different temperatures were used in the initial stage of the synthesis because the dissolution of Pluronics is highly temperature-dependent. A series of the samples was synthesized by changing the aging temperature (355 and 363 or 373 K), while keeping the same temperature during the initial stage of the synthesis to obtain samples with different microporosity. Moreover, for the P123 triblock copolymer, two different TEOS/copolymer molar ratios were applied: 60 (typical synthesis conditions) and 120 (TEOS excess route). It has been shown that the samples prepared using the TEOS excess route possess higher thermal stability,[11] which make them promising for catalytic applications because they can withstand the conditions used in industrial processes. The kind of niobium source was suggested by our previous studies, which showed that the use of niobium oxalate as Nb source favors the formation of NbO$^-$ in NbMCM-41 materials.[12] The structural and textural properties of Nb–MS were characterized by using different methods such as low- and high-angle X-ray diffraction (XRD), electron microscopy (TEM), nitrogen adsorption, temperature-programmed reduction (TPR), and energy-dispersive X-ray fluorescence (EDX).

Experimental Section

Synthesis. Nb–MS materials were prepared using tetraethyl orthosilicate (TEOS) (Aldrich) and niobium(V) oxalate (CBMM, Brazil) as silicon and niobium sources, respectively. The Si/Nb atomic ratio in the gel was kept at 64 for all the syntheses presented in this paper (samples with a higher niobium load were also prepared but they are not discussed here due to the presence of a high amount of extra-framework niobium species). The Pluronics were obtained as a gift from BASF Corp. (Poland and Belgium). The details regarding the composition and physical properties of the triblock copolymers used are summarized in Table 1 on the basis of manufacturer data and ref 13.

* Corresponding author. E-mail: jaroniec@kent.edu.
† Kent State University.
‡ A. Mickiewicz University.

Polymer-Templated Mesoporous Silicas Containing Nb

J. Phys. Chem. B, Vol. 108, No. 12, 2004 **3723**

TABLE 1: Physicochemical Data for the Pluronic-type Copolymers Used in the Synthesis of Nb−MS Materials

Pluronic[a]	physical form	molecular weight	$(PO)_y$ (% PO)	$2(EO)_x$ (% EO)	T_c^b K	CMT[c] K	T_s^d K
L43 (PE 4300)	liquid	1750	19 (70%)	14 (30%)	313	∼308	340
L64 (PE 6400)	liquid/ paste	2900	30 (60%)	26 (40%)	333	301.5	338
P94 (PE 9400)	waxy solid	4600	47 (60%)	42 (40%)	no data	∼293	332
P103 (PE 10300)	waxy solid	4950	56 (66%)	38 (34%)	359	290	330
P105 (PE 10500)	waxy solid	6500	56 (50%)	74 (50%)	>363	287.5	330
P123 (PE 12300)	waxy solid	5800	70 (70%)	40 (30%)	363	285	328

[a] Note that another notation for Pluronics is used, especially in Europe, and is provided in brackets. [b] Cloud point temperature, manufacturer data at 1 wt %. [c] Critical micellization temperature, data from ref 13. [d] Stirring temperature.

In the typical synthesis process, a 0.54 g of triblock poly-(ethylene oxide)−poly(propylene oxide)−poly(ethylene oxide) BASF P123 was dissolved in ∼2 M HCl solution obtained by using 53 g of water and 10 cm³ of concentrated HCl. Then, a 2.25 g of TEOS (to achieve TEOS/copolymer molar ratio of 120) was added under vigorous stirring at different temperatures, T_s (see Table 1 for details), followed by the addition of niobium oxalate solution prepared by dissolution of niobium source in 0.1 M oxalic acid. The quantity of niobium was calculated to be 0.09 g to reach the Si/Nb atomic ratio of 64. The stirring was continued for 8 h, and then the resultant mixture was aged at 353 or 363 K for 16 h without stirring. The sample was recovered by filtration, washed with a copious amount of water, and dried at 333 K. After calcination at 823 K for 8 h in air, the mesoporous Nb−MS was finally obtained. Beside this method, the standard procedure reported by Stucky and co-workers[2] with the TEOS/copolymer ratio of 60 was employed: a 1 g sample of P123 was combined with 15 g of water mixed with 7 cm³ of 2 M HCl. Afterward, a 2 g sample of TEOS was added, and the obtained combination was stirred at 333 K for 8 h. The mixture was allowed to react at 353 or 373 K for 16 h. The precipitate was treated in the same manner as described above.

The samples used in this work are denoted as follows: NbP-T-R, where P is the Pluronic type, T is the aging temperature in K, and R is the TEOS/copolymer molar ratio.

Characterization. The quantitative chemical analyses were performed by using an energy-dispersive X-ray fluorescence (EDX) technique on a Shimadzu EDX 700 instrument. The X-ray diffraction (XRD) experiments were performed with a TUR-42 powder diffractometer using nickel-filtered copper Kα radiation (10 kV, 40 mA). The diffractograms were carried out in two 2Θ ranges: 1.0−10° and 4−60° with a step of 0.02° and 0.05°, respectively. The transmission electron micrographs (TEM) were taken on a JEOL-2000 operated at 80 keV. Nitrogen adsorption/desorption isotherms at 77 K were recorded using a Micromeritics ASAP 2010 instrument. Before measurements, the samples were outgassed at 573 K for 3 h in the degas port of the adsorption instrument. The volume of adsorbed N_2 was normalized to the standard temperature and pressure. The BET surface area was calculated with the cross-sectional area of the nitrogen molecule taken as 0.162 nm² by applying the BET equation for relative pressure between 0.05 and 0.20. The pore sizes (D) were obtained from the N_2 adsorption branch using the Barret-Joyner-Halenda (BJH) method with the corrected Kelvin equation.[14] Moreover, the α_s-plot analysis was performed for all obtained samples for the evaluation of microporosity.[15] In this method, nitrogen adsorption data are plotted versus the standard reduced adsorption α_s, where α_s is defined as the amount adsorbed on a reference adsorbent at a given relative pressure divided by the amount adsorbed at a relative pressure of 0.4. The external surface area was evaluated from the slope of the α_s-plot linear segment, which appears after the condensation step. The intercept of this linear segment was
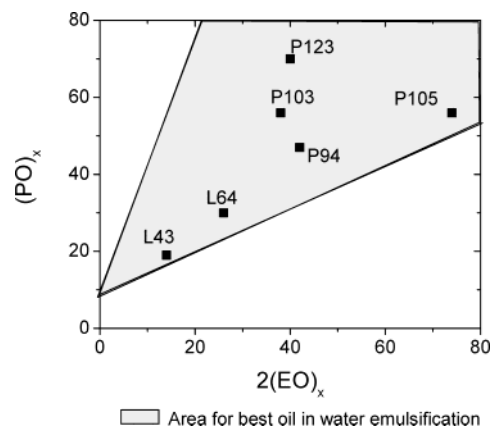

Figure 1. Phase diagram for Pluronic type triblock copolymers illustrating their behavior toward oil/water emulsification.

used to estimate the sum of the micropore and mesopore volumes, whereas the linear segment of the α_s-plot located before the condensation step was used to obtain the volume of micropores. The temperature-programmed reduction (H_2-TPR) of the Nb−MS materials was carried out using 10 vol % H_2 in Ar as a reducing agent with a flow rate of 32 cm³ min⁻¹ and a heating rate of 10 K min⁻¹ until 1373 K. The consumption of H_2 was monitored continuously with a thermal conductivity detector (Micromeritics PulseChemiSorb 2705).

Results and Discussion

As can be seen from Table 1, all the Pluronics used for the synthesis of the Nb−MS materials possessed the same percentage of poly(ethylene glycol) (30−40 wt %) in the polymer (with an exception of P105). However, two of the Pluronics used, L43 and L64, have a shorter EO chain than that essential for establishing the hexagonal structure and recommended by Alfredsson and co-workers,[16] i.e., 19−37 EO units. The above-mentioned Pluronics have a rather low cloud point, T_c, which could result in the formation of a lamellar phase.[17] All nonionic templates are the best water-in-oil emulsifiers, as evidenced in Figure 1.

The actual Si/Nb ratio in the calcined samples was determined to be the lowest for L43 (110), while the highest was for P105 (140) for the synthesis route employing TEOS excess. The others samples have the ratio of ∼125, thus the comparison of the structure was possible due to the small differences in the niobium loadings. The use of the conventional synthesis procedure for the preparation of Nb−MS materials led to about a twice lower amount of niobium incorporated. Under the synthesis conditions used in this work, only a part of niobium (∼50%) was incorporated into the final mesoporous material due to the strong acidic conditions during the synthesis procedure.

The typical powder XRD patterns for calcined Nb−MS samples show a hexagonal mesostructure for the samples
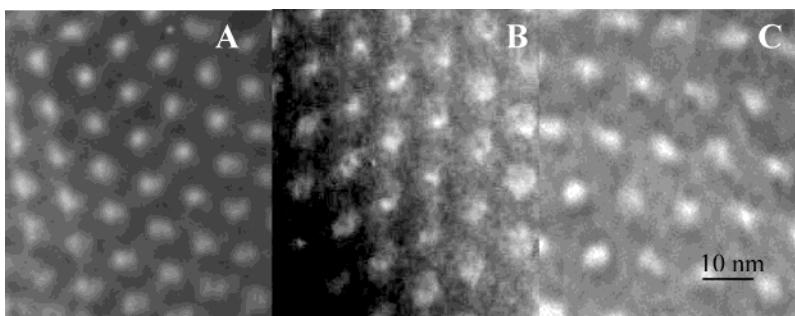
3724 *J. Phys. Chem. B, Vol. 108, No. 12, 2004*

Nowak et al.

Figure 2. Transmission electron micrographs for Nb94-353-120 (A), Nb105-353-120 (B), and Nb123-353-120 (C).

TABLE 2: Physicochemical Data for the Nb−MS Materials Obtained from EDX, XRD, and N_2 Adsorption

sample	Si/Nb ratio (real)	XRD unit- cell value a_0,[b] nm	BET surface area, $m^2 g^{-1}$	pore volume V_{total},[a] cm^3/g	pore width, D_{BJH}, nm	wall thickness, t,[b] nm
Nb43-353-120	110		680	0.47	2.0	
Nb64-353-120	113		760	0.43	3.9	
Nb94-353-120	123	9.2	610	0.44	4.7	4.5
Nb103-353-120	141	o	780	0.49	7.4	o
Nb105-353-120	137	9.6	610	0.44	5.7	3.9
Nb123-353-120	123	10.2	550	0.51	7.4	2.8
Nb123-353-60	239	10.6	780	0.62	7.5	3.1
Nb43-363-120	137		830	0.64	3.9	
Nb64-363-120	121		850	0.53	4.3	
Nb94-363-120	152	9.6	730	0.56	5.8	3.8
Nb103-363-120	125	o	830	0.72	7.4	o
Nb105-363-120	151	10.0	770	0.63	6.5	3.5
Nb123-363-120	158	10.6	730	0.78	8.6	2.0
Nb123-373-60	232	o	960	1.06	10.3	o

[a] Pore volume calculated from the amount adsorbed at $p/p_0 = 0.99$. [b]Wall thickness: $t = a_0 - D$; o indicates that the XRD unit cell was not measured for the sample but the sample mesostructural ordering was confirmed by TEM.

TABLE 3: Structural Properties of the Nb−MS Materials Studied Obtained by the α_s-Plot Analysis

sample	micropore volume V_{micro}, $cm^3 g^{-1}$	volume of ordered mesopores[a] V_{meso}, $cm^3 g^{-1}$	percentage of micropores	external surface area S_{ext}, $m^2 g^{-1}$
Nb43-353-120	0.14	0.16	47	90
Nb64-353-120	0.13	0.28	31	10
Nb94-353-120	0.12	0.27	30	10
Nb103-353-120	0.18	0.38	33	60
Nb105-353-120	0.14	0.26	35	20
Nb123-353-120	0.14	0.18	44	110
Nb123-353-60	0.19	0.37	34	50
Nb43-363-120	0.06	0.33	16	150
Nb64-363-120	0.06	0.45	11	20
Nb94-363-120	0.09	0.46	16	20
Nb103-363-120	0.17	0.46	27	60
Nb105-363-120	0.13	0.45	22	20
Nb123-363-120	0.17	0.22	43	230
Nb123-373-60	0.18	0.62	23	160

[a] The difference between the total pore volume assessed by nitrogen adsorption (see Table 2) and the sum of the micropore volume and the volume of ordered mesopores (see Table 3) denotes the volume of secondary mesopores.

prepared with P123, P105, P103, and P94 copolymers because two peaks were observed, which can be indexed on the hexagonal lattice as [110] and [200] reflections (see Figure S1 in Supporting Information). Because of large unit cell dimensions, the main [100] peak that appears to be located at angles below the lower angular limit of the powder diffractometer used was not recorded. Therefore, the unit cell was calculated from the [200] peak under the assumption that the interplanar spacing $d_{100} = 2d_{200}$. The unit cell parameter increases from 9.2 to 10.2 nm with increasing the Pluronic number and from 9.6 to 10.6 for samples prepared at 353 and 363 K, respectively (Table 2). The samples prepared with Pluronics L64 and L43 do not give any peaks on diffractograms that can be indexed as [110] and [200], thus suggesting low ordering of those materials. The TEM images (see Figure 2) recorded for the samples prepared with P123, P105, P103, and P94 triblock copolymers prove that the hexagonal structure was formed. This behavior was not dependent on the aging temperature. It is clearly visible that the samples prepared with lower Pluronic number possess a very high wall thickness. Although these materials have a high ordering of mesopores at the microscopic scale (see Figure 2), they have irregularly curved (U-shaped) pores at the macroscopic scale (not shown here). The formation of curve-shaped pores was especially evidenced for the samples prepared at higher aging temperature, i.e., 373 K. For the samples prepared with L64 and L43, more irregularly shaped pores were observed; this is reflected by a wormlike structure in the case of the latter sample.

In addition to the X-ray diffraction and transmission electron microscopy, which are commonly used to evaluate the structural

ordering of mesoporous materials,[18,19] gas adsorption is a technique of choice for evaluation of the pore size distribution, pore volume, and surface area of these materials.[20] The nitrogen adsorption/desorption isotherms for the samples prepared at lower aging temperature (353 K) by using P123, P105, P103, and P94 as templates were found to be type IV according to the IUPAC classification and exhibited different hysteresis loops with a steep condensation step, which is typical for mesoporous solids with uniform pore sizes. Figure 3A shows nitrogen adsorption isotherms at 77 K for the Nb−MS samples synthesized with different copolymers. All those materials exhibit a steep condensation step at different p/p_0. A decrease in the position of the inflection point of this step is observed with decreasing the cloud point with the exception of L43; however, in this case, the hexagonal phase was not formed as evidenced by XRD and TEM studies. The position of the inflection point is clearly related to the mesopore diameter, and the sharp condensation step reflects high uniformity of mesopores. Thus, Figure 3A shows the reduction of the mesopore size with decreasing the Pluronic number. For the samples prepared with P123 at 353 K, the isotherms show some pore blockage because the capillary evaporation was significantly delayed in relation to the capillary condensation. For the samples prepared at higher aging temperature (363 K), the formation of plugged mesopores was even more evident as seen in Figure 4A. To learn more about the state of the formed plugs, X-ray diffraction data at high angles ($2\Theta = 10-60°$) were collected. The measured data
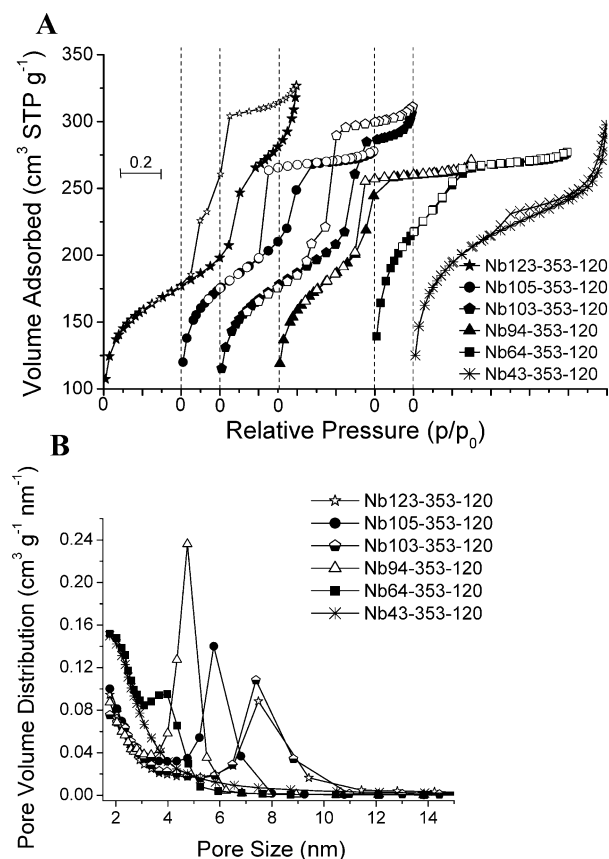
Polymer-Templated Mesoporous Silicas Containing Nb

J. Phys. Chem. B, Vol. 108, No. 12, 2004 **3725**

A

B

Figure 3. Nitrogen adsorption isotherms at 77 K and pore size distributions for the Nb−MS materials prepared at 353 K.

A

B

Figure 4. Nitrogen adsorption isotherms at 77 K and pore size distributions for the Nb−MS materials prepared at 363 K.

exhibit (see Figure S2 in Supporting Information) a signal corresponding to amorphous silica ($2\Theta = 16°$) and those of niobium(V) oxide phase ($2\Theta = 22.8$ and $28.5°$). This can suggest the formation of plugs with niobium oxide and/or silica in hexagonally templated silicas that was already suggested elsewhere[21,22] or some debris outside pores. It is worthy to add that for Nb123-363-120 a very high amount of extra-framework niobium was observed.

The pore size distribution (PSD) curves shown in Figure 3B are narrow for the samples prepared at lower aging temperature (i.e., 353 K). This is not the case when a higher temperature was used (Figure 4B). Moreover, the pore diameter is strongly dependent on the Pluronic number, which indicates the length of the poly(propylene oxide) chain. Yamada et al.[23] reported that the pore size of the SBA-15 materials is controlled by the micelle size. The relation between the pore size of the mesoporous silicate and the assembly conditions is the same as that for the radius of the triblock copolymer micelle, the solution temperature T_s, and the critical micellization temperature CMT (that can be estimated on the basis of ref 13, i.e., $r \sim (T_s-\text{CMT})^{0.2}$. Analogous behavior was observed in the case of our samples for which the pore diameter decreased with increasing the cloud point. As can be seen from Table 2 and Figures 5A,B, the pore size increases with increasing the molecular weight of triblock copolymer having the same percentage of EO groups in the following order: P123 > P103 > P94 > L64 > L43.

Surprisingly, the samples prepared with the use of P105 show smaller pore size than that of P103. Note that Alfredson and co-workers[16,24] did not observe the aforementioned behavior for the same group of triblock copolymers (P103, P104 and P105). Their data show almost no change in the pore diameters but they used different temperature and synthesis procedure. If one
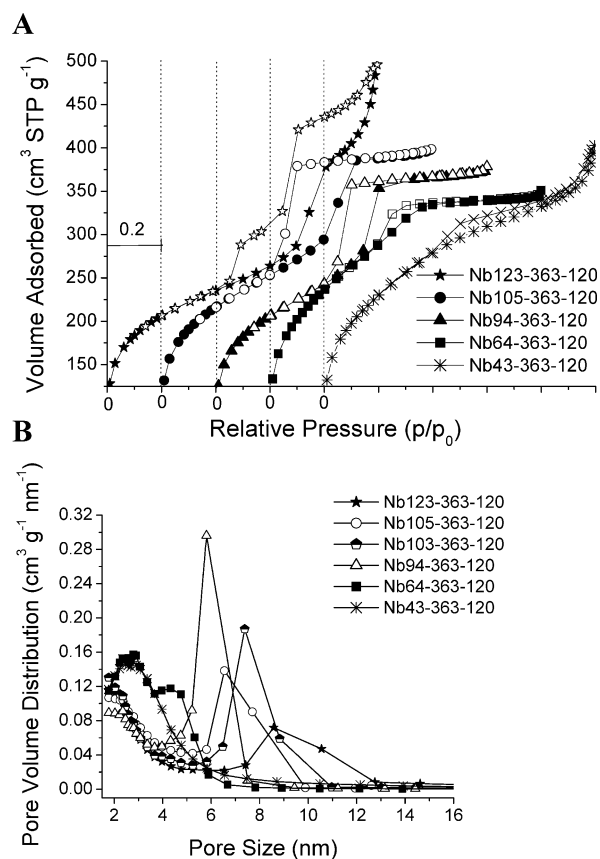
can consider that the mesopores are formed around the PO chains, then P103 possessing 66% of poly(propylene oxide) chains compared to 50% in P105 should give a larger pore diameter. This is in agreement with our observations. Recently, Flödstrom and Alfredsson[24] reported the synthesis at lower aging temperature, at which the pore diameter decreased from 4.4 nm for the P103 template to 3.3 nm for P105, which is expected on the basis of geometrical constraints.

Niobosilicas of the SBA-15-type made with P123 and P103 have slightly higher total pore volumes (around 0.50 cm^3 g^{-1}) than the materials prepared with other triblock copolymers ($\sim$0.45 cm^3 g^{-1}). The total pore volume increases with the aging temperature up to $\sim$0.8 cm^3 g^{-1} and 0.6 cm^3 g^{-1}, respectively. Unexpectedly, the highest mesopore volume and highest wall thickness ($\sim$4−5 nm) was obtained for the samples prepared with P94 (see Tables 2 and 3) that can imply the possible use of this material in catalysis. A comparable mesopore volume was obtained for the Nb103-353-120 and Nb103-363-120, i.e., samples prepared via excess TEOS route with Pluronic possessing a higher amount of PO$_x$ units than P94.

For the samples prepared at 353 K, the fraction of micropore volume is about 30−40% (Table 2 and Figure 5A) and the wall thickness decreases with increasing the pore diameter. An increase in the temperature from 353 to 363 K at the constant TEOS/Pluronic ratio caused a decrease in the micropore volume that is especially pronounced for the samples prepared with lower Pluronic number copolymers. This trend parallels the increase in the mesopore volume. The sample prepared at 373 K shows also a relatively small amount of micropores, which is in agreement with previous studies.[11,25]

The thickness of the walls is about 4−5 nm for the samples prepared at lower aging temperature (353 K). It decreases to

3726 *J. Phys. Chem. B, Vol. 108, No. 12, 2004*

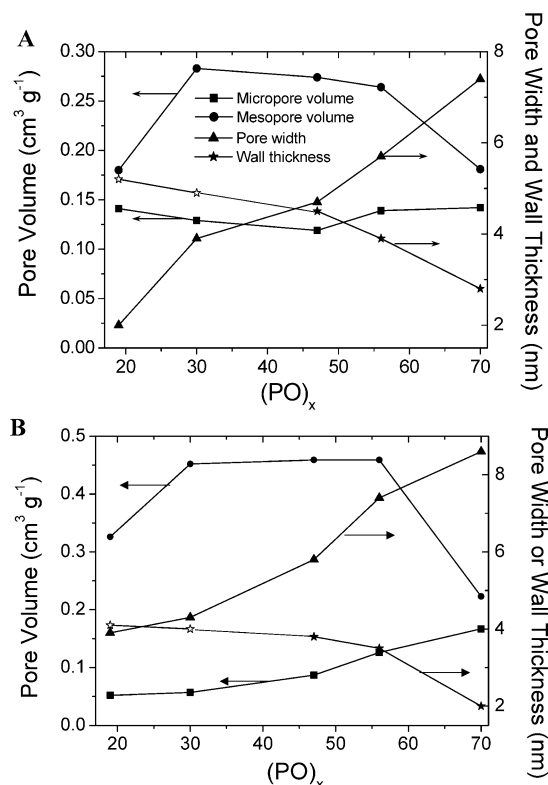Nowak et al.

A

B

Figure 5. Evolution of the micro- (●) /meso- (■) pore volumes, pore diameter (▲), and wall thickness (★, open symbols denote expected values) as a function of Pluronic type for the samples prepared at 353 (A) and 363 K (B).

Figure 6. TPR profiles for the Nb−MS samples.

about 3−3.4 nm for the samples prepared using P123. However, the temperature affected only slightly the wall thickness in the case of molecular sieves prepared using P103, P105, and P94. Moreover, the samples synthesized with P103 and P105 that have different PO chain length equal to 19 and 37, respectively, show different vales of the wall thickness and pore diameter. The first quantity increases with an increase in the EO chain length, whereas the second one decreases. The increase in the wall thickness was observed by Alfredsson and co-workers[24] when P103, P104, and P105 were applied for the syntheses of SBA-15 materials, whereas the pore diameter was constant. The later discrepancy between their results and ours was discussed above. In summary, for the samples studied, not only is microporosity affected by increasing temperature but also wall thickness. It is noteworthy that among the samples having ordered structure and made by using the TEOS/copolymer molar ratio of 120 only the materials made with P123 and P103 possessed very high external surface area, 110 and 60 m^2 g^{-1} and 230 and 60 m^2 g^{-1} at the synthesis temperatures of 353 and 363 K, respectively.

The H$_2$-TPR profiles for the Nb−MS samples prepared at 353 K are shown in Figure 6. It is known[12] that the low temperature (LT) peaks (below ~1000 K) are due to the reduction of extra-framework niobium species, whereas, those at high temperatures (above 1100 K) characterize the reduction of niobium localized in the framework. Up to six H$_2$-TPR peaks were registered for the sample prepared with P123, for which three of them at 960, 1030, and 1090 K can be assigned to the reduction of extra-framework niobium species, whereas the other three can be assigned to the framework niobium. Two of the TPR peaks, at 1280 and 1350 K, are like those observed for the niobosiliceous MCM-41 material (2D hexagonal mesostructure) and were assigned to NbO$^-$ and Nb$^+$
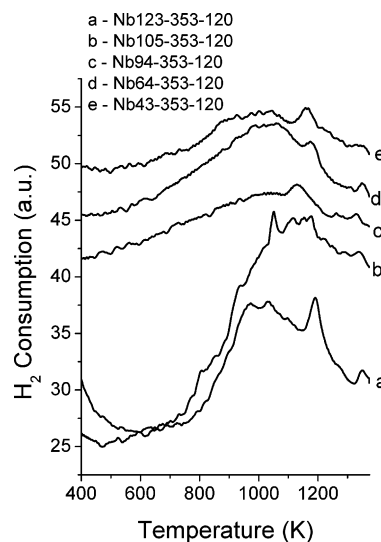
species connected with the silica terahedra.[26] An additional peak at 1180 K registered in Figure 6 can be assigned to the niobium species localized at a different environment than those niobium species present in NbMCM-41, as there are additional connections between the mesopores of the NbSBA-15 material, in which niobium can be settled. For other samples, the contribution of extra-framework niobium species was smaller with the favor for framework one. For the sample prepared with L43, only a small amount of niobium was incorporated in the structure, but this sample was poorly ordered.

It is noteworthy that the samples prepared with a higher niobium loading (not shown here) show lower adsorption as well as smaller microporosity in favor of mesoporosity. The average pore diameter increased with increasing the niobium amount introduced that can be explained by the formation of an extra-framework niobium species (TPR study not presented here).

The presented results demonstrate that control over the pore diameter, microporosity, and wall thickness of NbSBA-15 can be achieved using different types of triblock copolymers. There are potential applications of these materials in the oxidation processes in the gas phase due to their higher hydrothermal stability.

Supporting Information Available: Figures showing low-angle (Figure S1) and high-angle (Figure S2) XRD patterns for the NbSBA-15 samples synthesized by using Pluronic P123. This material is available free-of charge via the Internet at http://pubs.acs.org.

References and Notes

(1) Kresge, C. T.; Leonowicz, M. E.; Roth, W. J.; Vartuli, J. C.; Beck, J. S. *Nature* **1992**, *359*, 710; U.S. Patent 5,098,684, 1992; U.S. Patent 5,-102,643, 1992.

(2) Zhao, D.; Feng, J.; Huo, Q.; Melosh, N.; Fredrickson, G. H.; Chmelka, B. F.; Stucky, G. D. *Science* **1998**, *279*, 548.

(3) Kruk, M.; Jaroniec, M.; Ko, C. H.; Ryoo, R. *Chem. Mater.* **2000**, *12*, 1961.

(4) Lukens, W. W. Jr.; Schmidt-Winkel, P.; Zhao, D.; Feng, J.; Stucky, G. D. *Langmuir* **1999**, *15*, 403.

(5) Jung, Y. C.; Yoo, G. H.; Choo, W. J.; Ha, C. S. *Mol. Cryst. Liq. Cryst.* **2002**, *374*, 241.

(6) Lee, S. K.; Lee, J.; Joo, A.; Hyeon, T.; Ahn, W. S.; Lee, H. I.; Lee, C. H.; Choi, W. *J. Ind. Eng. Sci.* **2003**, *9*, 83.

(7) Zhang, W. H.; Lu, J. Q.; Han, B.; Li, M. J.; Xiu, J. H.; Ying, P. L.; Li, C. *Chem. Mater.* **2002**, *14*, 3413.

(8) Newalkar, B. L.; Olanrewaju, J.; Kamerneni, S. *J. Phys. Chem.* **2001**, *105*, 8356.

(9) Han, Y.; Xiao, F.-S.; Wu, S.; Sun, Y. Y.; Meng, X. J.; Li, D. S.; Lin, S.; Deng, F.; Ai, X. J. *J. Phys. Chem. B* **2001**, *105*, 7963.

(10) Han, Y.; Meng, X.; Guan, H.; Yu, R.; Zhao, L.; Xu, X.; Yang, X.; Wu, S.; Li, N.; Xiao, F.-S. *Microporous Mesoporous Mater.* **2003**, *57*, 191.

(11) Miyazawa, K.; Inagaki, S. *Chem. Commun.* **2000**, 2121.

(12) Ziolek, M.; Sobczak, I.; Lewandowska, A.; Nowak, I.; Decyk, P.; Renn, M.; Jankowska, B. *Catal. Today* **2001**, *70*, 169.

(13) Alexandridis, P.; Holzwarth, J. F.; Hatton, T. A. *Macromolecules* **1994**, *27*, 2414.

(14) Kruk, M.; Jaroniec, M.; Sayari, A. *Langmuir* **1997**, *13*, 6267.

(15) Jaroniec, M.; Kruk, M.; Olivier, J. P. *Langmuir* **1999**, *15*, 5410.

(16) Kipkemboi, P.; Fogden, A.; Alfredson, V.; Flodström, K. *Langmuir* **2001**, *17*, 5398.

(17) Zhang, K.; Khan, A. *Macromolecules* **1995**, *28*, 3807.

(18) Schacht, S.; Janicke, M.; Schuth, F. *Microporous Mesoporous Mater.* **1998**, *22*, 485.

(19) Thomas, J. M.; Terasaki, O.; Gai, P. L.; Zhou, W.; Gonzalez-Calbet, J. *Acc. Chem. Res.* **2001**, *34*, 583.

(20) Kruk, M.; Jaroniec, M. *Chem. Mater.* **2001,** *13,* 3169.

(21) van der Voort, P.; Ravikovitch, P. I.; De Jong, K. P.; Benjelloun, M.; van Bavel, E.; Janssen, A. H.; Neimark, A. V.; Weckhuysen, B. M.; Vansant, E. F. *J. Phys. Chem. B* **2002**, *106*, 5873.

(22) Kruk, M.; Jaroniec, M.; Joo, S. H.; Ryoo, R. *J. Phys. Chem. B* **2003**, *107*, 2205.

(23) Yamada, T.; Zhou, H.; Asai, K.; Honma, I. *Mater. Lett.* **2002**, *56*, 93.

(24) Flodström, K.; Alfredson, V. *Microporous Mesoporous Mater.* **2003**, *59*, 167.

(25) Galarneau, A.; Cambon, H.; Di Renzo, F.; Ryoo, R.; Choi, M.; Fajula, F. *Langmuir* **2001**, *17*, 8328; *New J. Chem.* **2003**, *27*, 73.

(26) Nowak, I.; Kilos, B.; Ziolek, M.; Lewandowska, A. *Catal. Today* **2003**, *78*, 487.